

An extended-cavity diode laser at 497 nm for laser cooling and trapping of neutral strontium

Vladimir Schkolnik[†] · Oliver Fartmann · Markus Krutzik

Abstract We present the first extended-cavity diode laser in Littrow configuration operating in the cyan wavelength range around 497 nm. The gallium-nitride based diode laser features a free-space output with up to 60 mW, operates in a single frequency mode, is tunable over a range of more than 8 nm and has a Lorentzian linewidth of less than 90 kHz. A detailed characterization of the tuning capabilities of the diode laser and its emission spectrum is provided. This compact, simple and low cost laser source replaces more complex systems based on frequency doubling and therefore simplifies the development of future compact and mobile optical clocks based on neutral strontium. Applications include efficient repumping of strontium atoms from the $5s5p\ ^3P_2$ state and the 9.8 MHz broad $5s5p\ ^3P_2 \rightarrow 5s5d\ ^3D_3$ transition might be of interest for sub-Doppler cooling.

1 Introduction

Nowadays, optical atomic clocks reach fractional uncertainties at the 2×10^{-18} level [1] and relative instabilities at the 10^{-17} level at one second of averaging time [2]. Due to their high accuracy and stability, optical clocks are used in various applications in fundamental research, pushing the limits in tests of the time variation of fundamental constants [3], tests of general relativity [4], search for dark matter [5,6] and are envisioned as detectors for gravitational waves [7]. Their high precision makes optical clocks also important tools for applications like navigation [8] and geodesy [9,10].

Vladimir Schkolnik · Oliver Fartmann · Markus Krutzik
Humboldt-Universität zu Berlin, Newtonstr. 15, 12489 Berlin, Germany
E-mail: vladimir.schkolnik@physik.hu-berlin.de

Currently the best performing optical clocks are based on neutral atoms trapped in a magic wavelength optical lattice [11]. In particular, clocks based on neutral strontium have become widely used over the world in the past, operating uninterrupted over multiple weeks in laboratories and recently started to even perform outside the lab [12].

However, the general scheme for laser cooling and trapping of neutral strontium and other alkaline earth atoms is more complex compared to the one used for alkali atoms [13]. The cooling process starts with a first cooling stage utilizing the broad $^1S_0 \rightarrow ^1P_1$ transition at 460.9 nm, from where atoms can decay towards the meta-stable 3P_2 state with a branching of roughly 1 in 50,000 (see Figure 1), which limits the MOT lifetime to a few tens of milliseconds [14]. To increase the number of atoms in the MOT several repumping schemes have been employed. Due to the availability of laser sources the majority of strontium lattice clocks use two repump lasers addressing the $^3P_2 \rightarrow ^3S_1$ transition at 707 nm

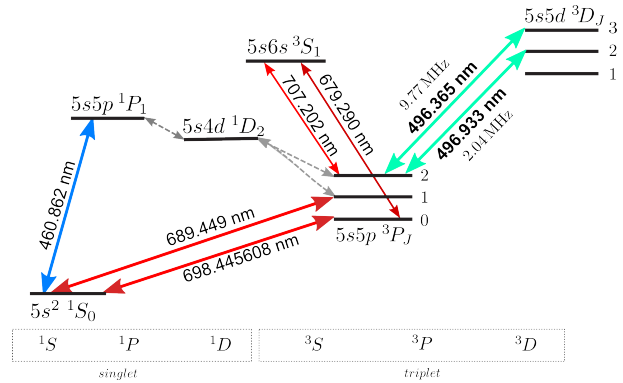


Fig. 1 The level scheme for the bosonic strontium isotope ^{88}Sr with transitions used for laser cooling, repumping, clock operation and detection and their vacuum wavelengths (linewidth given for the cyan transitions).

and the $^3P_0 \rightarrow ^3S_1$ transition at 679 nm. Alternatively, only a single repump laser addressing the $^3P_2 \rightarrow ^3D_2$ transition at 496.93 nm may be used [15, 16]. Until now the generation of light at this wavelength relied on second harmonic generation (SHG) from an infrared laser due to the lack of laser diodes directly operating in this range. This results in complex setups with low optical output power but high power consumption that are undesirable for mobile applications.

Newly available gallium-nitride (GaN) laser diodes operating around 495 nm pave the way to build extended-cavity diode lasers (ECDL) at 497 nm. This allows for more compact and energy efficient laser sources for laser cooling and trapping of strontium. Optical powers of up to 100 mW open up the possibility of sub-Doppler cooling on the almost closed cycling transition $^3P_2 \rightarrow ^3D_3$ [14, 17] as already successfully demonstrated with the alkaline earth metal calcium [18]. This could lead to temperatures in the μK regime, sufficient for effectively loading atoms into the magic wavelength lattice and therefore allows to replace the usual laser system at 689 nm that requires prestabilization to an optical cavity.

Here we present the first laser source at 497 nm based on an extended-cavity diode laser in Littrow configuration. After presenting the characteristics of the used laser diodes in Chapter 2.1 we present the ECDL design in Chapter 2.2, followed by the characterization of its tuning and spectral characteristics in Chapter 2.3 and 2.4, respectively. We conclude with an outlook on future applications in Chapter 3.

2 Extended-cavity diode laser at 497 nm

2.1 Laser diodes

In the past years GaN diodes covering the spectrum from 370 nm to 530 nm have become commercially available. For applications using neutral strontium atoms, diodes operating around the 460 nm transition reach output powers of up to 100 mW (Nichia corporation, NDB4216), and with amplifier chips multiple thereof should be available in the near future. Diodes based on InAlGaN multiple quantum wells for the wavelength region around 495 nm and 500 nm, tunable to the $^3P_2 \rightarrow ^3D_2$ and $^3P_2 \rightarrow ^3D_3$ transition in neutral strontium at 496.36 nm and 496.93 nm, respectively, were recently introduced from Sharp (GH04955A2G) [19]. According to the data sheet the emission wavelength of these non AR-coated diodes spans from 480 nm to 495 nm. For our purposes we use diodes from a selected batch with a peak wavelength of 495 nm.

2.2 ECDL design

The design of our diode laser is shown in Figure 2. It consists of an extended-cavity diode laser in Littrow configuration [20] and a mirror for angle compensation [21]. Light emitted from the laser diode is collimated using an aspheric lens with a focal length $f = 4.02$ mm. The collimated light from the diode illuminates a holographic reflective grating (Thorlabs, GH13-24V) and the -1^{st} order is being reflected back into the laser diode providing the optical feedback. The reflected 0^{th} order is used as the output. The grating period d of 24001/mm results in a diffraction angle of 36.5° . The diffraction efficiency in the -1^{st} order is about 38 % and about 44 % are reflected into the 0^{th} order.

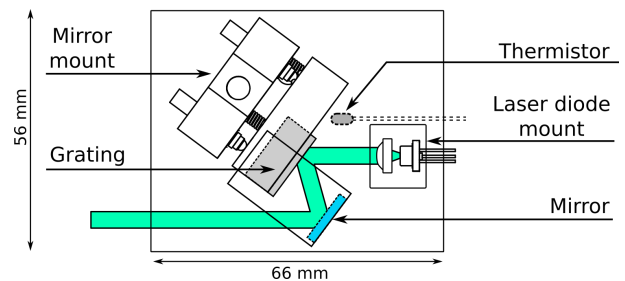


Fig. 2 Top-view schematic of the extended-cavity diode laser. The Peltier element underneath the base plate (outer frame in the picture) is not shown.

The laser diode is mounted in a press fit aluminum mount inspired by the laser pointer community. This ensures good thermal contact between the diode and the rest of the assembly. The grating is embedded into a mirror mount (Radiant Dyes, MNI-H-U-2-3000) to reduce the cavity length and thus to increase the stability. Both the mirror mount and the diode mount are integrated onto a small aluminium base plate. The temperature is stabilized using a digital TEC controller (Meerstetter Engineering, TEC-1091) by means of a Peltier element and an NTC thermistor that is positioned in the base plate between the diode and the grating, inspired by [22]. The diode mount and the mirror mount are fixed with nylon screws and finally glued to the base plate. A mirror is mounted on a small lever parallel to the grating to compensate for the angle change of the beam due to wavelength tuning with the grating angle [21]. Our diode laser current source is based on the Libbrecht-Hall design [23]. 86 % of laser emission passes an optical isolator (LINOS, FI-488-3SC) and is coupled into a polarization-maintaining optical fiber with an efficiency of ≈ 55 % for optical spectrum analysis.

2.3 Power and tuning characteristics

We measured the output power of the bare laser diode and of the assembled ECDL both at a temperature of 25 °C. The power was measured before the optical isolator. The results are shown in Figure 3. According to the data sheet, the absolute maximum injecting current is 135 mA with a typical output power of 55 mW at 105 mA. In our measurement, we operated the laser diode at injection currents up to 200 mA. As can be seen from Figure 3, the output power of the free running diode reaches 127 mW with only a slight deviation from a linear current/power relationship of 5.9%. Therefore, an output power of almost 2.5 times as high as the maximum stated rating is achieved. No thermal roll-over could be observed for even higher injection currents up to 500 mA, which we address to a good thermal contact of the laser diode to the heatsink, resulting in an enhanced temperature stabilization of our compact setup. At 500 mA, we measured an optical power of 242 mW.

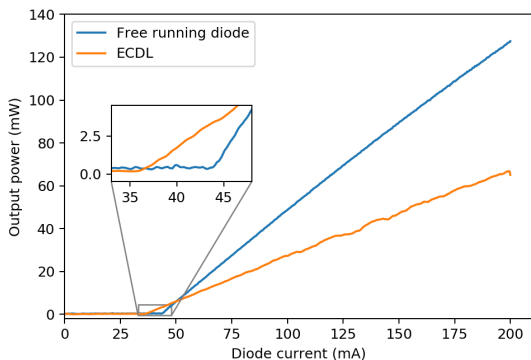


Fig. 3 The output power of the bare laser diode (blue) and of the ECDL with optical feedback from the grating (orange) as a function of the injection current at 25 °C. The inset shows the reduced laser threshold of the ECDL.

In the ECDL configuration the output power reaches 65 mW at an injection current of 200 mA and the lasing threshold is reduced from 44 mA to 36 mA compared to the free running configuration. We are not concerned about the back reflected power from the grating since it is not a major source of diode damage for GaN diodes, as in the case for GaAs diodes [24]. The high output power of this ECDL is useful for a wide range of applications such as laser cooling and spectroscopy at cyan wavelengths around 495 nm, where only SHG sources could deliver comparable power levels so far. The power could be further increased by injection locking a second diode in a master slave configuration. To further investigate the suitability of our laser source for

atomic physics, wavelength tuning range and the laser linewidth are investigated.

The wavelength of the ECDL is tuned by changing the grating angle. Figure 4 shows the emission spectra of our ECDL for different wavelengths along with the emission spectrum of the bare diode (grey shadowed), measured with an optical spectrum analyzer (OSA). All measurements were performed at an injection current of 105 mA and at a diode temperature of 25 °C. A tuning range of ≈ 8 nm around the center wavelength, covering the range from 491 nm to 499 nm is achieved. This is comparable to commercial diode laser systems in the visible part of the spectrum and, to our knowledge, the first tunable diode laser covering this part of the spectrum.

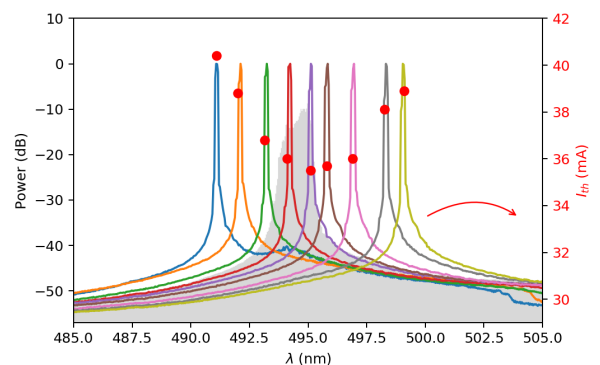


Fig. 4 Optical spectra of the ECDL for different wavelengths accessible with our configuration (colored) and for laser diode without feedback (grey) measured at 25 °C. The red data points show the lasing threshold for each ECDL spectrum.

The resolution of the measurement is limited by our OSA to 0.1 nm. The lasing threshold for each of the spectra is also shown in Figure 4. It is strongly reduced compared to the bare diode and is the smallest for the wavelength of 495 nm, the peak wavelength of the bare diode.

2.4 Emission linewidth

The power output of the ECDL is sufficient for laser spectroscopy and cooling applications with neutral strontium as has been shown above. Another criteria for the suitability of a laser in atomic physics is the linewidth. It should be narrower than the linewidth of the transition we want to address, in our case 2.04 MHz for the $^3P_2 \rightarrow ^3D_2$ transition at 496.93 nm.

To investigate the linewidth of the diode laser we assembled a second laser and measured the free running beat note between both of them. Figure 5 shows

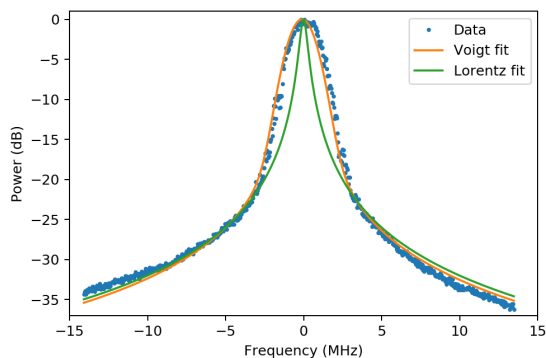


Fig. 5 Analysis of the beat note between two lasers for a sweep time of 400 ms averaged for 35 sweeps. For a single laser this results in a Lorentzian linewidth of 88 kHz and a Gaussian linewidth of 1.22 MHz. See text for more details.

the analysis of our beatnote measurement where 35 sweeps were averaged for better statistics. Fitting a Voigt model to the data yields a Lorentzian linewidth of 175(1) kHz and a Gaussian linewidth of 1.72(1) MHz at a sweep time of 400 ms. The Lorentzian linewidth is divided by 2 and the Gaussian linewidth is divided by $\sqrt{2}$ to obtain the respective linewidths of a single laser. The resulting Lorentzian linewidth of 88 kHz is comparable to commercial diode laser systems in the visible part of the spectrum. The Gaussian linewidth of 1.22 MHz stems from external influences and from possible noise in our current driver and temperature controller. The linewidth could therefore be further reduced by low noise electronics and an improved laser housing that is less susceptible to mechanical and acoustic vibrations. Even without further improvement, the linewidth is already lower than the linewidths of the transitions in neutral strontium around 497 nm.

3 Conclusion

We built and characterized an extended-cavity diode laser operating in the cyan wavelength range around 497 nm. The laser provides an optical output power of 65 mW at 200 mA with only a slight deviation from a linear current/power relationship. A tuning range of ≈ 8 nm around the centre wavelength of 495 nm was achieved. The linewidth of the laser was determined to be 88 kHz for the Lorentzian part and 1.22 MHz for the Gaussian part.

This compact, simple and low cost laser source can be used for several applications. Laser systems for cooling of strontium atoms can be considerably simplified in two different ways. First, the laser source can be utilized as a repump laser at 496.93 nm to replace pre-

vious more complex systems and to reduce the number of needed laser sources. Second, sub-Doppler cooling at 496.36 nm can be employed to replace the second cooling stage at 689 nm. Furthermore these laser source facilitates quantum computing schemes using the $^3P_2 \rightarrow ^3D_3$ transition at 496.36 nm for population detection [25], can be used for experimental investigation of the highly forbidden $5s \rightarrow 6s$ transition in rubidium and potentially for compact optical frequency standards taking advantage of cyan transitions in molecular iodine [26]. Lastly, experiments employing cold barium ions can profit from convenient diode lasers for the cooling transition $6s^2S_{1/2} \rightarrow 6p^2P_{1/2}$ at 493.5 nm [27].

Acknowledgements This work is supported by the DLR Space Administration with funds provided by the Federal Ministry for Economic Affairs and Energy (BMWi) under grant numbers DLR 50WM1753 and 1857.

The Authors would like to thank Achim Peters for useful discussions and providing resources, Klaus Döringshoff for useful discussions and proofreading the manuscript.

References

1. T. Nicholson, S. Campbell, R. Hutson, G. Marti, B. Bloom, R. McNally, W. Zhang, M. Barrett, M. Safronova, G. Strouse, W. Tew, and J. Ye, “Systematic evaluation of an atomic clock at 2×10^{-18} total uncertainty,” *Nature Communications*, vol. 6, p. 6896, dec 2015.
2. C. Sanner, N. Huntemann, R. Lange, C. Tamm, E. Peik, M. S. Safronova, and S. G. Porsev, “Optical clock comparison test of Lorentz symmetry,” sep 2018.
3. M. S. Safronova, S. G. Porsev, C. Sanner, and J. Ye, “Two Clock Transitions in Neutral Yb for the Highest Sensitivity to Variations of the Fine-Structure Constant,” *Physical Review Letters*, vol. 120, no. 17, p. 173001, 2018.
4. V. Dzuba and V. Flambaum, “Limits on gravitational Einstein equivalence principle violation from monitoring atomic clock frequencies during a year,” *Physical Review D*, vol. 95, p. 015019, jan 2017.
5. B. M. Roberts, G. Blewitt, C. Dailey, M. Murphy, M. Pospelov, A. Rollings, J. Sherman, W. Williams, and A. Derevianko, “Search for domain wall dark matter with atomic clocks on board global positioning system satellites,” *Nature Communications*, vol. 8, p. 1195, dec 2017.
6. T. Kalaydzhyan and N. Yu, “Extracting dark matter signatures from atomic clock stability measurements,” *Physical Review D*, vol. 96, p. 075007, oct 2017.
7. S. Kolkowitz, I. Pikovski, N. Langellier, M. Lukin, R. Walsworth, and J. Ye, “Gravitational wave detection with optical lattice atomic clocks,” *Physical Review D*, vol. 94, p. 124043, dec 2016.
8. S. Schiller, A. Gorlitz, A. Nevsky, S. Alighanbari, S. Vasilyev, C. Abou-Jaoudeh, G. Mura, T. Franzen, U. Sterr, S. Falke, C. Lisdat, E. Rasel, A. Kulosa, S. Bize, J. Lodewyck, G. M. Tino, N. Poli, M. Schioppo, K. Bongs, Y. Singh, P. Gill, G. Barwood, Y. Ovchinnikov, J. Stuhler, W. Kaenders, C. Braxmaier, R. Holzwarth, A. Donati, S. Lecomte, D. Calonico, and F. Levi, “The space optical clocks project: Development of high-performance transportable and breadboard optical clocks and advanced sub-

- systems,” in 2012 European Frequency and Time Forum, pp. 412–418, IEEE, apr 2012.
9. T. E. Mehlstäubler, G. Grosche, C. Lisdat, P. O. Schmidt, and H. Denker, “Atomic clocks for geodesy,” Reports on Progress in Physics, vol. 81, p. 064401, jun 2018.
 10. J. Flury, “Relativistic geodesy,” Journal of Physics: Conference Series, vol. 723, p. 012051, jun 2016.
 11. A. D. Ludlow, M. M. Boyd, J. Ye, E. Peik, and P. Schmidt, “Optical atomic clocks,” Reviews of Modern Physics, vol. 87, pp. 637–701, jun 2015.
 12. J. Grotti, S. Koller, S. Vogt, S. Häfner, U. Sterr, C. Lisdat, H. Denker, C. Voigt, L. Timmen, A. Rolland, F. N. Baynes, H. S. Margolis, M. Zampaolo, P. Thoumany, M. Pizzocaro, B. Rauf, F. Bregolin, A. Tampellini, P. Barbieri, M. Zucco, G. A. Costanzo, C. Clivati, F. Levi, and D. Calonico, “Geodesy and metrology with a transportable optical clock,” Nature Physics, vol. 14, pp. 437–441, may 2018.
 13. H. J. Metcalf and P. van der Straten, “Laser cooling and trapping of atoms,” Journal of the Optical Society of America B, vol. 20, p. 887, may 2003.
 14. S. Stellmer and F. Schreck, “Reservoir spectroscopy of $5s\ 5p\ 3P\ 2 - 5s\ n\ d\ 3D\ 1, 2, 3$ transitions in strontium,” Physical Review A, vol. 90, p. 022512, aug 2014.
 15. P. H. Moriya, M. O. Araújo, F. Todão, M. Hemmerling, H. Keßler, R. F. Shiozaki, R. C. Teixeira, and P. W. Courteille, “Comparison between 403 nm and 497 nm repumping schemes for strontium magneto-optical traps,” arXiv, jun 2018.
 16. N. Poli, R. E. Drullinger, G. Ferrari, J. Léonard, F. Sorrentino, and G. M. Tino, “Cooling and trapping of ultracold strontium isotopic mixtures,” Physical Review A - Atomic, Molecular, and Optical Physics, vol. 71, no. 6, pp. 1–4, 2005.
 17. Y. Hayakawa, T. Sato, C. Watanabe, T. Aoki, and Y. Torii, “Doppler-free spectroscopy of metastable Sr atoms using a hollow cathode lamp,” Applied Optics, vol. 57, p. 1450, feb 2018.
 18. J. Gruünert and A. Hemmerich, “Sub-Doppler magneto-optical trap for calcium,” Physical Review A. Atomic, Molecular, and Optical Physics, vol. 65, no. 4, pp. 414011–414014, 2002.
 19. “Sharp product lineup.” Accessed: 2018-01-16.
 20. L. Ricci, M. Weidemüller, T. Esslinger, A. Hemmerich, C. Zimmermann, V. Vuletic, W. König, and T. Hänsch, “A compact grating-stabilized diode laser system for atomic physics,” Optics Communications, vol. 117, pp. 541–549, jun 1995.
 21. C. J. Hawthorn, K. P. Weber, and R. E. Scholten, “Littrow configuration tunable external cavity diode laser with fixed direction output beam,” Review of Scientific Instruments, vol. 72, pp. 4477–4479, dec 2001.
 22. S. D. Saliba, M. Junker, L. D. Turner, and R. E. Scholten, “Mode stability of external cavity diode lasers,” Applied Optics, vol. 48, p. 6692, dec 2009.
 23. K. G. Libbrecht and J. Hall, “A low-noise high-speed diode laser current controller,” Review of Scientific Instruments, vol. 64, pp. 2133–2135, aug 1993.
 24. J. W. Tamm, R. Kernke, G. Mura, M. Vanzi, and M. Hempel, “Comparison of catastrophic optical damage events in GaAs- and GaN-based diode lasers,” in 2017 IEEE High Power Diode Lasers and Systems Conference (HPD), pp. 55–56, IEEE, oct 2017.
 25. A. J. Daley, J. Ye, and P. Zoller, “State-dependent lattices for quantum computing with alkaline-earth-metal atoms,” European Physical Journal D, vol. 65, no. 1-2, pp. 207–217, 2011.
 26. W.-Y. Cheng, L. Chen, T. H. Yoon, J. L. Hall, and J. Ye, “Sub-Doppler molecular-iodine transitions near the dissociation limit (523–498 nm),” Optics Letters, vol. 27, p. 571, apr 2002.
 27. D. Hucul, J. E. Christensen, E. R. Hudson, and W. C. Campbell, “Spectroscopy of a Synthetic Trapped Ion Qubit,” Physical Review Letters, vol. 119, p. 100501, sep 2017.